

RESEARCH

Open Access



# Long noncoding RNA SNHG1 promotes TERT expression by sponging miR-18b-5p in breast cancer

Yujuan Kang<sup>1†</sup>, Lin Wan<sup>1†</sup>, Qin Wang<sup>1</sup>, Yanling Yin<sup>1</sup>, Jiena Liu<sup>1</sup>, Lei Liu<sup>1</sup>, Hao Wu<sup>1</sup>, Lei Zhang<sup>1</sup>, Xin Zhang<sup>1</sup>, Shouping Xu<sup>1\*</sup> and Da Pang<sup>1,2\*</sup> 

## Abstract

**Background:** Long noncoding RNA (lncRNA) small nucleolar RNA host gene 1 (SNHG1) plays a positive role in the progression of human malignant tumors. However, the molecular mechanism of SNHG1 remains elusive in breast cancer.

**Results:** LncRNA SNHG1 was upregulated and had a positive relationship with poor prognosis according to bioinformatics analysis in pan-cancer including breast cancer. Silencing SNHG1 inhibited tumorigenesis in breast cancer both in vitro and in vivo. Mechanistically, SNHG1 functioned as a competing endogenous RNA (ceRNA) to promote TERT expression by sponging miR-18b-5p in breast cancer. miR-18b-5p acted as a tumor repressor in breast cancer. Moreover, the combination of SNHG1 knockdown and TERT inhibitor administration showed a synergistic inhibitory effect on breast cancer growth in vivo. Finally, E2F1 as a transcription factor, binding to SNHG1 promoter and enhanced SNHG1 transcription in breast cancer.

**Conclusions:** Our results provide a comprehensive understanding of the oncogenic mechanism of lncRNA SNHG1 in breast cancer. Importantly, we identified a novel E2F1–SNHG1–miR-18b-5p–TERT axis, which may be a potential therapeutic target for breast cancer. Our results also provided a potential treatment for breast cancer when knock-down SNHG1 and TERT inhibitor administration simultaneously.

**Keywords:** SNHG1, TERT, Breast cancer, Competing endogenous RNA, E2F1

## Background

Long noncoding RNAs (lncRNAs) are a large family of RNAs with limited protein-coding potential, length of over 200 nucleotides, and lack of a detectable open reading frame [1–5]. Importantly, lncRNA dysregulation has been observed in various cancers, and they reportedly participate in cancer cell growth, metastasis, and drug resistance [6, 7]. Moreover, lncRNAs are a novel class of

potential biomarkers and therapeutic targets for cancer treatment [8]. In terms of regulatory mechanisms, when lncRNAs are located in the nucleus, they regulate gene expression by acting as epigenetic modulators [9, 10]; whereas, most lncRNAs in the cytoplasm harbor multiple binding sites for identical microRNAs (miRNAs), and are called competing endogenous RNAs (ceRNAs) [11]. miRNAs are a class of pervasive, conserved, small, noncoding RNAs that act as negative gene regulators to repress the expression of target genes [12]. ceRNAs can sequester miRNAs and protect the target mRNAs from being repressed [13, 14]. LncRNA small nucleolar RNA host gene 1 (SNHG1) is localized at 11q12.3 and shows upregulated expression in various cancers, including

\*Correspondence: Shoupingxu@hrbmu.edu.cn; pangda@ems.hrbmu.edu.cn

<sup>†</sup>Yujuan Kang and Lin Wan contributed equally to this work

<sup>1</sup> Department of Breast Surgery, Harbin Medical University Cancer Hospital, Harbin 150040, China

Full list of author information is available at the end of the article



glioma and lung cancer [15–17]. In addition, SNHG1 reportedly serves as an oncogene in human cancers including breast cancer [18]. For instance, Cui et al. have shown that SNHG1 promotes the progression of pancreatic cancer via the Notch-1 signaling pathway [19]. Pei et al. has showed that interference SNHG1 inhibited the differentiation of Treg cells by promoting miR-448 expression and regulating IDO level, thereby impeding the immune escape of breast cancer [20]. Xiong et al. showed that SNHG1 promotes breast cancer progression by regulating of LMO4 [21]. Li et al. SNHG1 activates HOXA1 expression via sponging miR-193a-5p in breast cancer progression [22]. Zheng et al. SNHG1 contributes to proliferation and invasion by regulating miR-382 in breast cancer [23].

Telomeres are cellular nucleoprotein complexes that maintain chromosomal integrity and genome stability [24]. Telomeres are formed by hexameric repeats of a 5'-TTAGGG-3' sequence ending in a 3' single-stranded overhang, the G-strand overhang [25, 26] that protects the genomic DNA from the continued erosion of telomeres during cell division. Human telomerase is composed of two main core subunits: TERT, which constitutes the catalytic subunit and telomerase RNA component, which provides a template for telomerase elongation [27–29]. Human TERT protein levels are rate-limiting for telomerase activity and telomere length homeostasis [30]. A positive correlation between TERT mRNA expression and telomerase activity has been observed, thereby suggesting that telomerase is primarily regulated by TERT gene expression [28, 31, 32]. In approximately 90% of human tumors, telomerase is either upregulated or reactivated to maintain the telomeres during numerous rounds of cell divisions that are required for the emergence of malignant and metastatic diseases [33]. In cancer cells, TERT activity shows differential upregulation that is possibly due to several processes, such as transcriptional regulation, alternate RNA splicing, and post-translational modifications such as protein phosphorylation [30, 34]. Breast cancer is one of the leading mortal causes from cancer among women worldwide [35, 36]. Surgery, radiotherapy, chemotherapy and hormone therapy are still the main and common therapeutic approaches to treat breast cancer [37]. It was reported that the mRNA expression

of TERT in breast cancer samples has a positive relationship with poor prognosis [38]. However, to date, no studies have determined the mechanism of the relationship between SNHG1 and TERT in breast cancer. Thus, in this study, we attempted to elucidate the oncogenic function of SNHG1 in breast cancer. To the best of our knowledge, this is the first study to report that a E2F1–SNHG1–miR-18b-5p–TERT axis is involved in breast cancer, and this axis may be a novel potential therapeutic target for the same. Moreover, the combination of SNHG1 knockdown and TERT inhibitor administration may be a potential treatment for breast cancer.

## Results

### Expression of SNHG1 was upregulated in cancerous tissues and positively related to poor prognosis

To determine the expression level of SNHG1 in human pan-cancer tissues, TCGA data was downloaded and analyzed. SNHG1 expression level was higher in thyroid carcinoma (THCA), stomach adenocarcinoma (STAD), sarcoma (SARC), rectum adenocarcinoma (READ), prostate adenocarcinoma (PRAD), pheochromocytoma and paraganglioma (PCPG), lung squamous cell carcinoma (LUSC), lung adenocarcinoma (LUAD), liver hepatocellular carcinoma (LIHC), kidney renal papillary cell carcinoma (KIRP), kidney renal clear cell carcinoma (KIRC), kidney chromophobe (KICH), head and neck squamous cell carcinoma (HNSC), esophageal carcinoma (ESCA), colon adenocarcinoma (COAD), cholangiocarcinoma (CHOL), cervical squamous cell carcinoma and endocervical adenocarcinoma (CESC), breast invasive carcinoma (BRCA) (Additional file 3: Table S1), bladder urothelial carcinoma (BLCA) than in normal tissues (Fig. 1a and Additional file 4: Table S2). Furthermore, the expression of SNHG1 was also more upregulated in pan-cancer tissues than in normal tissues (Fig. 1b). We also examined five pairs of breast cancer tissues and normal breast tissues to determine SNHG1 expression and observed that SNHG1 showed higher expression level in breast cancer tissues than in paired normal tissues (Fig. 1c and Additional file 5: Table S3). The PrognScan database demonstrated that higher expression level of SNHG1 was associated with poor relapse-free survival (RFS) (Fig. 1d), and disease-specific survival (DSS) (Fig. 1e) in patients

(See figure on next page.)

**Fig. 1** Expression of SNHG1 was upregulated in cancerous tissues and positively related to poor prognosis. **a** The Cancer Genome Atlas results showed that the expression level of SNHG1 was higher in THCA, STAD, SARC, READ, PRAD, PCPG, LUSC, LUAD, LIHC, KIRP, KIRC, KICH, HNSC, ESCA, COAD, CHOL, CESC, BRCA, BLCA than in normal tissues. **b** Expression level of SNHG1 was also higher in pan-cancer tissues than in normal tissues. **c** Expression level of SNHG1 was higher in breast cancer tissues than in normal tissue (N = 5 per group). **d, e** PrognScan results showed that higher SNHG1 expression level had a positive association with poor overall survival (OS), relapse-free survival (RFS), and disease-specific survival (DSS) in breast cancer. **f, g** Higher expression level of SNHG1 was related to poorer OS and DSS according to pan-cancer analysis. \* $P < 0.05$ ; \*\* $P < 0.01$ ; \*\*\* $P < 0.001$ ; \*\*\*\* $P < 0.0001$ ; NS no significance

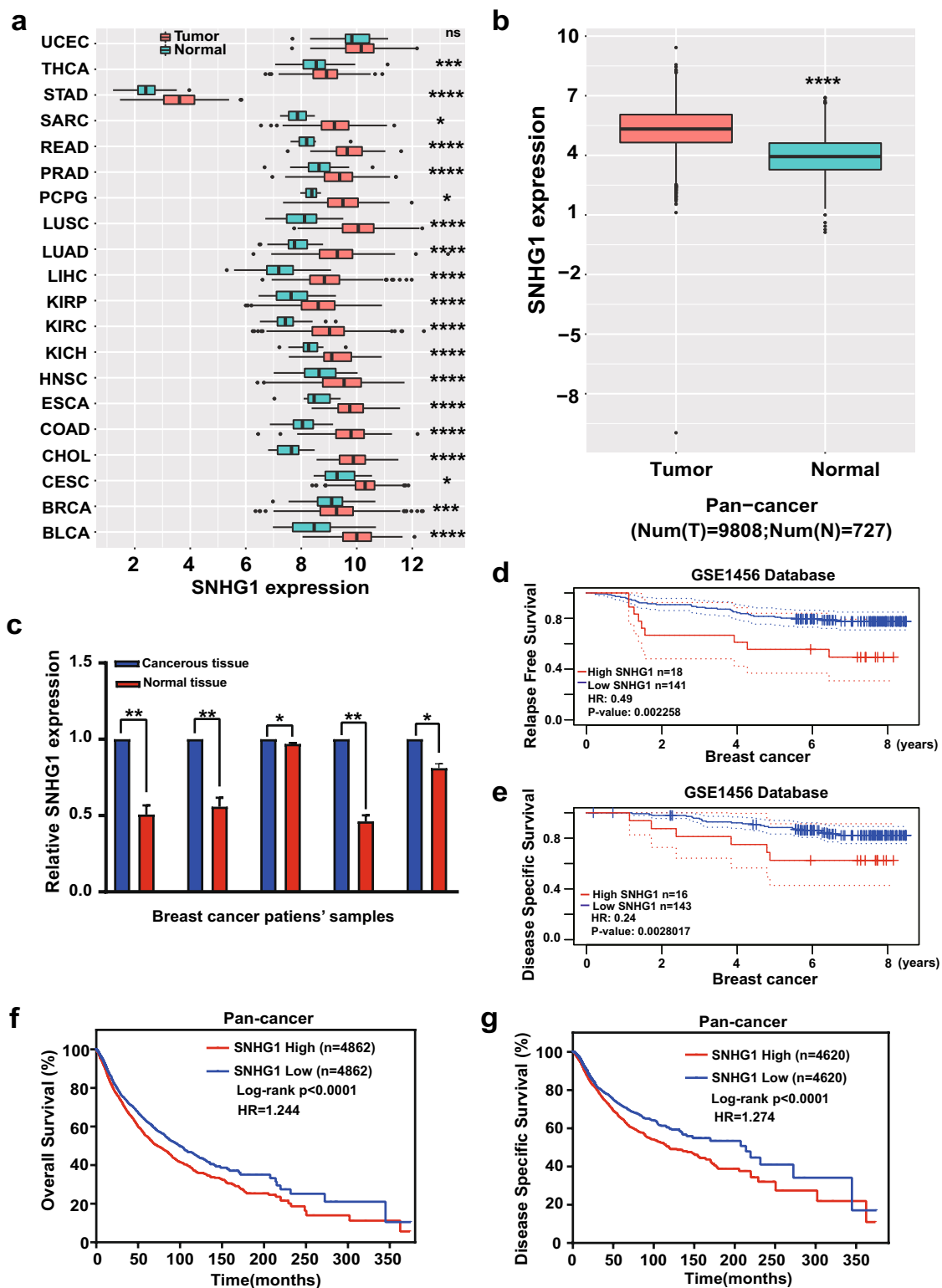


**Fig. 1** (See legend on previous page.)

with breast cancer. In pan-cancer analysis, upregulated SNHG1 expression was also related to poor overall survival (OS) and DSS (Fig. 1f, g, Additional file 4: Table S2). Moreover, higher expression of SNHG1 also correlated with poor prognosis in UCEC, LIHC, PRAD, and adrenocortical carcinoma (ACC) (Additional file 1: Fig. S1a–k and Additional file 4: Table S2). We use the KM plotter (<http://kmplot.com/analysis/>) to evaluate the prognostic value of SNHG1 in different cancers [39]. Higher expression of SNHG1 was correlated with poor OS in LIHC, KIRC, SARC and UCEC (Additional file 1: Fig. S1l–o).

### SNHG1 as an oncogene promoted tumorigenesis both in vitro and in vivo

Hs578T, MDA-MB-468, and MDA-MB-231 are breast cancer cell lines that have higher SNHG1 expression level than MCF10A cells (Fig. 2a); consequently, they were chosen for subsequent experiments. SNHG1 was knocked down by transfection with siSNHG1, and the transfection efficiency of siSNHG1 was evaluated using reverse transcription-polymerase chain reaction (RT-PCR) (Fig. 2b). Further, cell counting kit-8 (CCK-8), colony formation, wound healing, and Transwell invasion assays were performed to identify the function of SNHG1 in breast cancer. We observed that silencing of SNHG1 inhibited tumor cell proliferation, colony formation and suppressed tumor cell migration and invasion (Fig. 2c–f).

Subsequently, we evaluated the functions of SNHG1 in vivo. Lentivirus was synthesized to construct a 4T1 stable knockdown of *snhg1* (sh-*snhg1*). Knockdown efficiency was determined using RT-PCR, and we observed that the virus could knockdown *snhg1* in 4T1, as expected (Fig. 2g). The CCK-8 assay showed that the sh-*snhg1* group had poorer proliferation ability than the scramble group (Fig. 2h). Further, 4T1 scramble and 4T1 sh-*snhg1*#3 cells were subcutaneously injected into Balb/C female mice. As expected, the mice from the sh-*snhg1*#3 group had smaller tumors than those from the scramble group (Fig. 2i), thereby suggesting that SNHG1 acted as an oncogene in vivo as well. Moreover, the median tumor weight in the sh-*snhg1*#3 group was lower than that in the control group (Fig. 2j). The tumorigenesis

and tumor tissue of each group of Balb/C mice are shown as Fig. 2k. Furthermore, we pay attention to the relationship between SNHG1 expression and survival. The animal experiment results showed that sh-*snhg1*#3 group mice have a longer survival compared with scramble group (N=8) (Fig. 2l). Thus, the abovementioned results showed that SNHG1 acted as an oncogene in breast cancer both in vitro and in vivo.

### SNHG1 boosted TERT expression

Then, TCGA data was downloaded to evaluate the correlation between SNHG1 and TERT in pan-cancer and breast cancer. The results showed that TERT is positively correlated with SNHG1 in pan-cancer scope (R=0.2945) and breast cancer scope (R=0.3685) (Fig. 3a, b and Additional file 6: Table S4). In addition, the Gene Expression Profiling Interactive Analysis (GEPIA) was used to verify this relationship, and the results showed that TERT was positively correlated with SNHG1 (Fig. 3c).

Moreover, according to SNHG1 gene expression level, BRCA cancer tissue samples were divided into two groups: SNHG1 high expression group and SNHG1 low expression group. We identified a total of 595 differential expressed genes (FDR<0.01, fold change>1.2), among which 456 genes were upregulated and 139 genes were downregulated (Fig. 3d, e and Additional file 7: Table S5). TERT gene was upregulated expressed between high group and low group with FDR=4.45785008467688e-19, FC=0.418132443350429. As TERT was a certain target gene of SNHG1 in breast cancer, we select it as the SNHG1 downstream gene.

The GEPIA database showed that TERT expression level was considerably higher in breast cancer tissues than in normal tissues (Fig. 3f). Just as Fig. 3g showed, TERT presents a higher expression level in breast cancer cell lines than in MCF10A cell. We then examined four pairs of breast cancer tissues and normal breast tissues to determine TERT expression and observed that TERT showed higher expression level in breast cancer tissues than in paired normal tissues (Fig. 3h and Additional file 5: Table S3). Moreover, CCK-8, colony formation and wound healing assays were performed to identify

(See figure on next page.)

**Fig. 2** SNHG1 acts as an oncogene promoted tumorigenesis both in vitro and in vivo. **a** Expression of SNHG1 in MCF10A, Hs578T, MDA-MB-231, and MDA-MB-468 cell lines. **b** Transfection efficacy of siSNHG1 in MDA-MB-468, Hs578T, and MDA-MB-231 cells. **c** CCK-8 showed that silencing SNHG1 inhibited tumor cell proliferation. **d** Colony formation assay showed that silencing SNHG1 inhibited tumor cell clone formation. **e** Wound healing assay proved that silencing SNHG1 suppressed tumor cell migration. **f** Transwell invasion assay showed that knockdown of SNHG1 inhibited the invasion ability of tumor cells. **g** Knockdown efficacy of lentiviral targeting of *snhg1*. **h** CCK-8 showed that silencing of *snhg1* suppressed 4T1 proliferation. **i** Tumor growth curve of mice shows that sh-*snhg1*#3 group had slower growth than that in the scramble group. **j** Tumor weight in the sh-*snhg1*#3 group was lower than that in the scramble group. **k** The tumorigenesis and tumor tissue of each group of Balb/C mice (N=6 per group) are shown. **l** The survival of scramble and sh-*snhg1*#3 mice (N=6 per group). Data are presented as the mean value from three independent experiments  $\pm$  S.D. \* $P < 0.05$ ; \*\* $P < 0.01$ ; \*\*\* $P < 0.001$ ; \*\*\*\* $P < 0.0001$ ; NS no significance

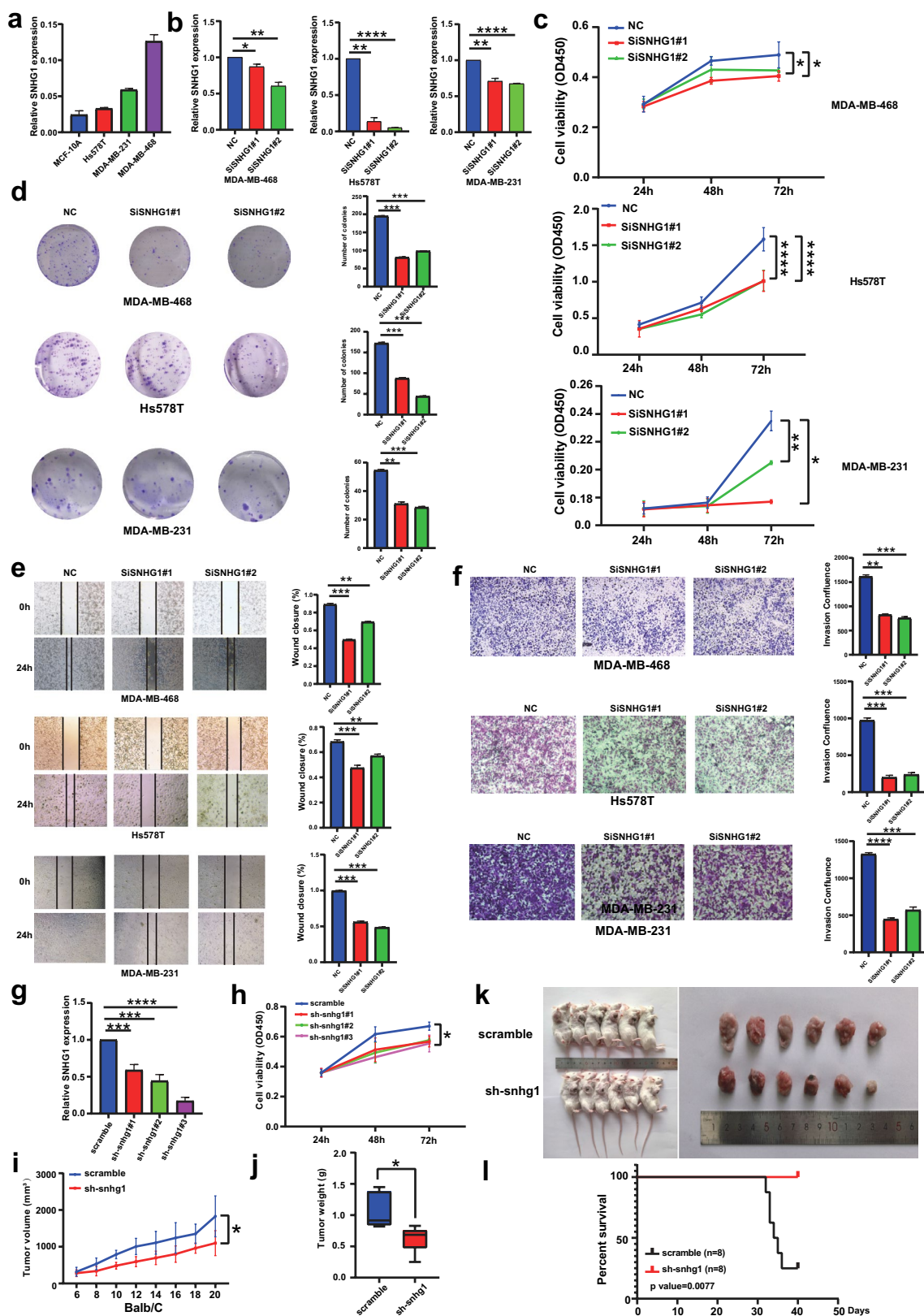


**Fig. 2** (See legend on previous page.)

the function of TERT in breast cancer. We observed that silencing of TERT inhibited tumor cell proliferation and colony formation and tumor cell migration ability (Additional file 2: Fig. S2a–c).

SiSNHG1 was transfected into MDA-MB-468 and Hs578T, and RT-PCR was used to examine the transfection efficiency of siSNHG1 (Fig. 3i). Consequently, we observed that knockdown of SNHG1 downregulated the expression of TERT at both RNA (Fig. 3j) and protein levels (Fig. 3k) in MDA-MB-468 and Hs578T cells in comparison to their levels in corresponding control groups. To validate the regulatory axis through a contrasting approach, we also transfected SNHG1 overexpression plasmid to MDA-MB-468 and Hs578T. RT-PCR was used to confirm the transfection efficiency (Fig. 3l). The expression of TERT in RNA and protein level is upregulated in SNHG1 overexpression group compared to control group (Fig. 3m, n). Furthermore, for the in vivo experiment, we extracted protein and RNA from mouse tumors and observed that the expression level of TERT in mouse tumors was lower in the sh-snhg1#3 group than in the control group (Fig. 3o).

Thus, SNHG1 promoted TERT expression in breast cancer. Next, we wondered whether targeting SNHG1 and TERT could produce a synergistic inhibitory effect. BIBR1532 is a nonnucleotidic small molecule compound that selectively inhibits telomerase activity by competitively binding to the active site of hTERT [40]. As we expected, the combination of knocking down snhg1#3 and administering the BIBR1532 (TERT inhibitor) prohibited tumor growth more powerfully than either approach alone (Fig. 3p, q). The median weight in the combination group was lower than that in the snhg1 knockdown group or control group (Fig. 3r).

#### miR-18b-5p acted as a tumor suppressor in breast cancer

We further explored the mechanism by which SNHG1 promoted the expression of TERT in breast cancer.

First, LncLocator was used to predict the subcellular localization of SNHG1, and the results showed that SNHG1 was mainly localized in the cytoplasm (Fig. 4a). Then, a cytoplasmic-nuclear RNA fractionation kit was used to confirm the forward prediction results in HEK293T, MDA-MB-468, and Hs578T cells (Fig. 4b). Both methods implied that SNHG1 was mainly localized in the cytoplasm. Therefore, we hypothesized that cytoplasmic SNHG1 might regulate TERT mRNA by acting as a ceRNA of miRNAs. To confirm this hypothesis, we used miRbase, TargetScan, and starBase databases to predict the possible miRNAs that could interact with both SNHG1 and TERT, simultaneously (Additional file 8: Table S6). The intersection of miRNAs acquired from these databases revealed 15 overlapping miRNAs (Fig. 4c). RT-PCR was used to determine the upregulated miRNAs after silencing SNHG1 in MDA-MB-468 and Hs578T cells (Fig. 4d, e). Finally, miR-18b-5p and miR-383-5p were chosen for subsequent experiments. However, when miR-383-5p mimics were transfected into Hs578T cells, the expression of TERT was upregulated (Fig. 4f). Thus, miR-18b-5p was the only candidate for subsequent experiments. Moreover, after SNHG1 overexpression, the expression of miR-18b-5p also downregulated when compared with control group in MDA-MB-468 and Hs578T (Fig. 4g). To explore the functions of miR-18b-5p in breast cancer, we performed CCK-8, colony formation, wound healing, and Transwell invasion assays by transfecting Hs578T, MDA-MB-468, and MDA-MB-231 cells with miR-18b-5p mimics. The transfection efficiency of miR-18b-5p mimics was verified by RT-PCR (Fig. 4h), and cell proliferation and colony formation were attenuated on transfecting miR-18b-5p mimics (Fig. 4i, j). Further, wound healing and Transwell invasion assays showed that overexpression of miR-18b-5p could inhibit tumor cell migration and invasion (Fig. 4k, l). Thus, the above-mentioned experiments indicated that miR-18b-5p may act as a tumor suppressor in breast cancer.

(See figure on next page.)

**Fig. 3** SNHG1 boosted TERT expression. TCGA data showed that TERT is positively correlated with SNHG1 in pan-cancer (N = 9725) (a) and in breast cancer (N = 1097) (b). c GEPIA showed that TERT expression level was higher in breast cancer tissues than in normal tissues. d, e We identified that TERT gene was upregulated expressed between high SNHG1 group and low SNHG1 group with FDR = 4.45785008467688e-19, FC = 0.418132443350429 in breast cancer. f GEPIA showed that the expression of TERT a higher level in breast cancer tissue than that in normal tissue. g TERT presents a higher expression level in breast cancer cell lines than in MCF10A cell. h TERT showed higher expression level in breast cancer tissues than in paired normal tissues in our own cohort (N = 4 per group). i Transfection efficacy of siSNHG1. j Knockdown of SNHG1 downregulated TERT mRNA expression in Hs578T and MDA-MB-468 cells. Knockdown of SNHG1 also downregulated TERT protein expression in MDA-MB-468 and Hs578T cells (k). l The transfection efficiency of SNHG1 plasmid. m, n The expression of TERT RNA and protein upregulated after SNHG1 overexpression. o TERT protein had a higher expression level in the scramble group than in the sh-snhg1#3 group. p–r The tumorigenesis, tumor tissue, tumor growth and tumor weight of 4T1 cells in each group of Balb/C mice (N = 6 per group) are shown. Data are presented as the mean value from three independent experiments ± S.D. \*P < 0.05; \*\*P < 0.01; \*\*\*P < 0.001; \*\*\*\*P < 0.0001; NS no significance

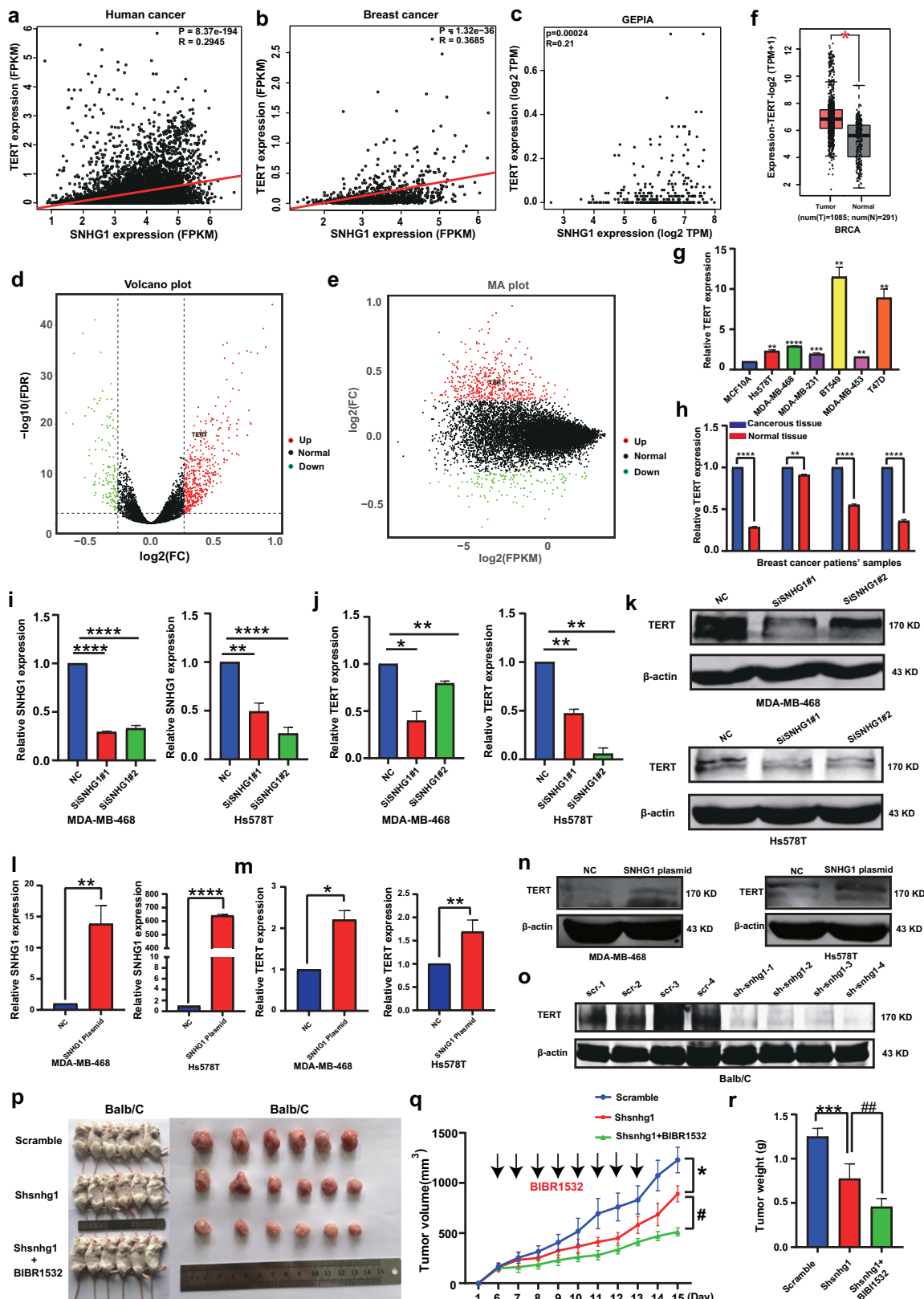


**Fig. 3** (See legend on previous page.)

### SNHG1 acted as a ceRNA to enhance TERT expression by sponging miR-18b-5p

We further explored the regulatory mechanism of SNHG1, miR-18b-5p, and TERT in breast cancer. RT-PCR was used to evaluate the transfection efficiency of miR-18b-5p mimics (Fig. 5a). TERT RNA level was downregulated after transfecting miR-18b-5p mimics (Fig. 5b); whereas, the TERT RNA level was upregulated after transfecting miR-18b-5p inhibitor (Fig. 5d). Accordingly, TERT protein level was downregulated after transfecting miR-18b-5p mimics (Fig. 5c), and upregulated after transfecting miR-18b-5p inhibitor (Fig. 5e). Furthermore, overexpression of miR-18b-5p inhibited SNHG1 expression; however, downregulation of miR-18b-5p promoted SNHG1 expression in MDA-MB-468 and Hs578T cells (Fig. 5f, g). Moreover, silencing SNHG1 and inhibiting miR-18b-5p weakened the downregulation of TERT protein level in MDA-MB-468 and Hs578T cells (Fig. 5h). Finally, the dual-luciferase reporter assay was used to demonstrate the binding relationship between SNHG1, miR-18b-5p, and TERT. As expected, wild-type 3'-untranslated region of TERT was regulated by miR-18b-5p, and this effect could be neutralized by mutating the binding sites in the luciferase reporter (Fig. 5i). Additionally, we obtained similar results for the regulation of SNHG1 (Fig. 5j). SNHG1 function was partially mediated by inhibiting miR-18b-5p in breast cancer cells. We transfected siSNHG1 and miR-18b-5p inhibitor into breast cancer cells and observed that siSNHG1-mediated restraint in cell proliferation and invasion abilities could be partially rescued by co-transfection of miR-18b-5p inhibitor in Hs578T and MDA-MB-468 cells (Fig. 5k, l). In addition, the expression of miR-18b-5p was more upregulated in Balb/C mice with snhg1 knockdown than in the scramble group ( $N=5$ ) (Fig. 5m), which was consistent with our previous conclusion. Thus, SNHG1 upregulated the expression of TERT via a ceRNA mechanism by sponging miR-18b-5p in breast cancer.

### E2F1 promoted SNHG1 transcription

We further focused on elucidating the upstream transcription regulation mechanism of SNHG1. First, PROMO database was used to predict potential

transcription factors (TFs) that could bind to the SNHG1 promoter (Additional file 9: Table S7). We focused on E2F1, a prominent TF that mediates transcriptional activation in a variety of tumors. TCGA data was downloaded to evaluate the correlation between E2F1 and SNHG1 in pan-cancer and breast cancer. The results showed that E2F1 is positively correlated with SNHG1 in pan-cancer ( $R=0.4129$ ) and breast cancer ( $R=0.3521$ ) (Fig. 6a and Additional file 10: Table S8). To verify this prediction, we transfected MDA-MB-468, Hs578T, and HEK293T cells with an siRNA to silence E2F1. Knockdown efficiency was examined by RT-PCR (Fig. 6b) and western blotting analysis (Fig. 6c). RT-PCR showed that the expression level of SNHG1 (Fig. 6d) and TERT (Fig. 6e) in the siE2F1 group was lower than that in the control group. Moreover, the expression of miR-18b-5p is increased after silencing E2F1 (Fig. 6f). Further, the JASPAR database was used to predict the potential binding site between E2F1 and SNHG1 promoter (Fig. 6g, h, Additional file 11: Table S9). Finally, chromatin immunoprecipitation-PCR assay indicated that in comparison with the Mock group, E2F1 was enriched at the SNHG1 promoter in Hs578T and HEK293T cells (Fig. 6i). Overall, we found a regulatory axis, E2F1–SNHG1–miR-18b-5p–TERT, play a vital role in breast cancer. Then, we found that when silencing TERT in MDA-MB-468 and Hs578T, the expression of SNHG1 decreased and the expression of miR-18b-5p upregulated. There may be a circle regulation mechanism between SNHG1 and TERT in breast cancer which deserved to excavate in the future (Fig. 6j, k). A schematic illustration of this study is shown in Fig. 6l.

### Discussion

Numerous studies have highlighted the functions of these regulatory lncRNAs in many biological processes, such as cancer development, stem cell differentiation, and chemotherapy resistance [41]. For instance, lncHOST2 act as a sponge of let-7b, thus increasing STAT3 expression and leading to breast cancer tumorigenesis [42]. SNHG1 promotes tumor growth by regulating the transcription of both local and distal genes [43]. TERT boosts epithelial-mesenchymal

(See figure on next page.)

**Fig. 4** miR-18b-5p acted as a tumor suppressor in breast cancer. **a** LncLocator predicted the subcellular localization of SNHG1. **b** Subcellular RNA fraction confirmed that SNHG1 was mainly located in the cytoplasm in HEK293T, MDA-MB-468, and Hs578T cells. **c** The intersection of TargetScan and StarBase predicted miRNAs. **d, e** The upregulated miRNAs after silencing of SNHG1 in MDA-MB-468 and Hs578T cells. **f** Expression of TERT after transfecting miR-383-5p mimics in Hs578T cells. **g** The expression of miR-18b-5p was downregulated after SNHG1 overexpression. **h** Transfection efficiency of miR-18b-5p mimics in Hs578T, MDA-MB-468, and MDA-MB-231 cells. **i** Colony counting kit-8 proved that miR-18b-5p inhibited cell proliferation. **j–l** Colony formation assay, wound healing assay and Transwell invasion assay showed that miR-18b-5p inhibited breast cancer cell colony formation, migration and invasion. Data are presented as the mean value from three independent experiments  $\pm$  S.D. \* $P < 0.05$ ; \*\* $P < 0.01$ ; \*\*\* $P < 0.001$ ; \*\*\*\* $P < 0.0001$ ; NS no significance

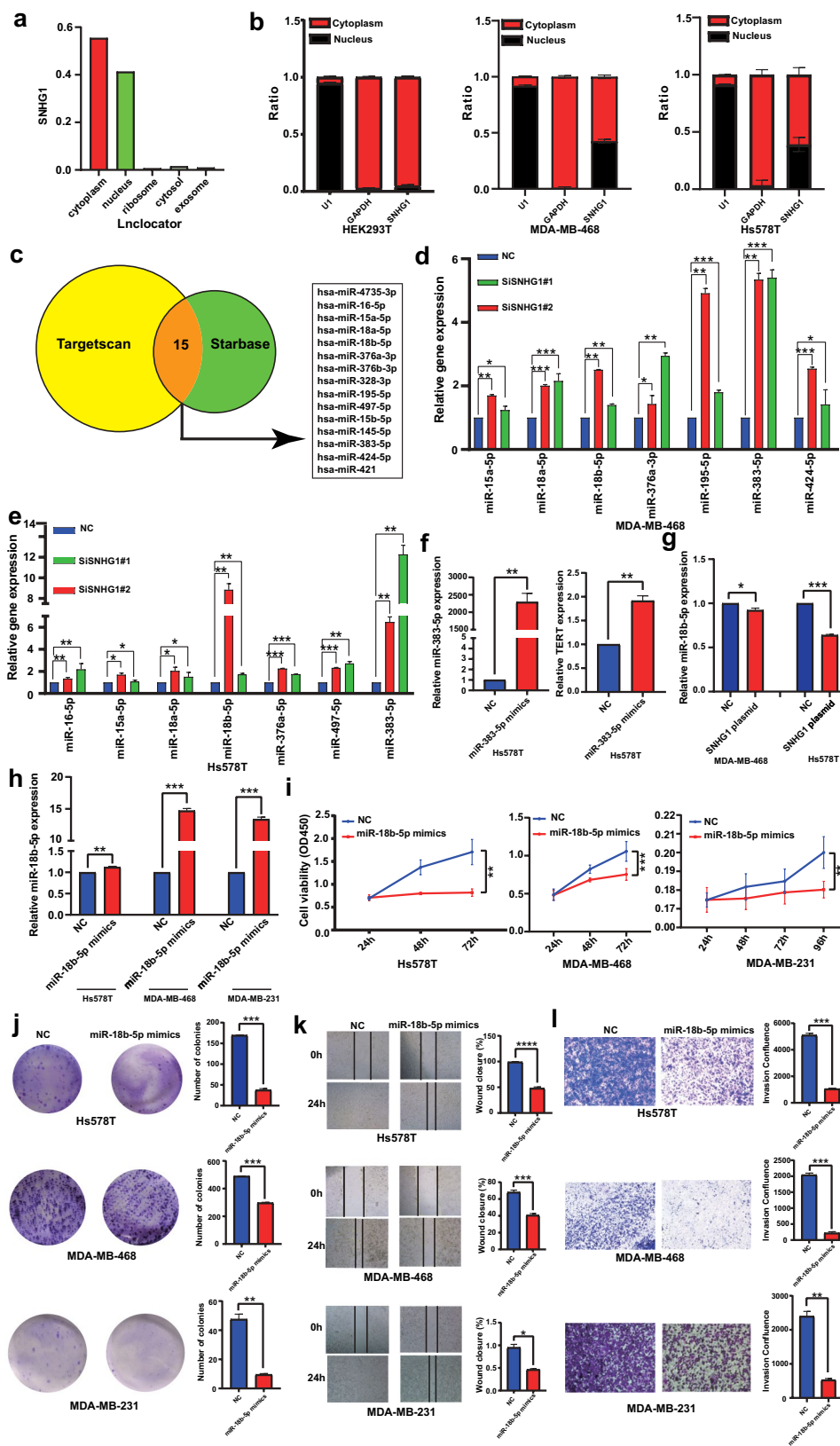


**Fig. 4** (See legend on previous page.)

transformation and stemness, thereby indicating an important role in cancer progression [44]. This study revealed that SNHG1 was an oncogene that promoted the expression of TERT in breast cancer.

When lncRNAs are in the cytoplasm, they participate in modulating mRNA stability, regulating mRNA translation, serving as ceRNAs, and functioning as precursors of miRNAs [45]. Here, subcellular fractionation confirmed that SNHG1 was mainly located in the cytoplasm in breast cancer cell lines implying that SNHG1 acted as a ceRNA to enhance TERT expression by sponging miR-18b-5p in breast cancer.

To further explore the tumorigenesis mechanism of SNHG1 in breast cancer, we explored the upstream regulation of SNHG1. Notably, we observed that E2F1 could bind to the SNHG1 promoter and enhance its transcription in breast cancer. To summarize, this study uncovered a novel mechanistic axis, E2F1–SNHG1–miR-18b-5p–TERT, in breast cancer tumorigenesis, and this axis may be a potential therapeutic target for breast cancer. In addition, the combination of SNHG1 knockdown and TERT inhibitor administration showed a synergistic inhibitory effect on breast cancer growth which may provide a potential therapy for clinical therapy for breast cancer in near future. However, our study also has some limitations. Firstly, TERT might only be one of the many targets of miR-18b-5p and other targets gene should also be studied in future. Secondly, we have not studied the regulatory mechanism of SNHG1 which located in nucleus, and we will continue this study in near future. Thirdly, although SNHG1 was associated with shortened patients' survival, it remains unclear if it can predict prognosis independent of other clinicopathological parameters, including age, sex and TNM staging.

## Conclusions

Our results identified a novel E2F1–SNHG1–miR-18b-5p–TERT axis, which may be a potential therapeutic target for breast cancer.

## Methods

### Public data access and analysis

Genome-wide SNHG1 expression profile and clinical pathology information for human cancers were downloaded from TCGA database (<https://tcga-data.nci.nih.gov/>). The transcript SNHG1 was normalized by log<sub>2</sub> transformation. The expression of SNHG1 was dichotomized using a study-specific median expression as the cutoff to define “high value” at or above the median versus “low value” below the median. The detailed clinical pathological information including ID number, TNM stage of breast cancer patient from TCGA is shown in Additional file 3: Table S1. GEPIA database (<http://gepia.cancer-pku.cn/>) and TCGA database were used to predict the correlations between SNHG1 and TERT; E2F1 and SNHG1 in pan-cancer and breast cancer. Correlations between genes were assessed by Pearson correlation coefficients. Prognoscan (<http://dna00.bio.kyutech.ac.jp/PrognoScan/index.html>) [46] and KM plotter (<http://kmplot.com/analysis/>) were used to examine the survival of breast cancer patients according to differential SNHG1 expression level. The expression profile of coding gene in breast cancer was extracted from TCGA BRCA expression profile (Additional file 7: Table S5). According to SNHG1 expression level, breast cancer tissue samples were divided into two groups. SNHG1 high expression group was found to be more than or equal to the median value of SNHG1, while SNHG1 low expression group was found to be less than the median value. Differentially expressed gene (DEG) was identified by edgeR between SNHG1 high expression and low expression group, of which FDR < 0.01, FC > 1.2.

### Cell culture

MDA-MB-468, Hs578T, HEK293T, MDA-MB-231 and 4T1 cell lines were obtained from the Chinese Academy of Sciences Cell Bank. MDA-MB-468, Hs578T, HEK293T and 4T1 were cultured with DMEM medium (Gibco, Waltham, MA) and 10% fetal bovine serum (FBS; Gibco), 100 µ/mL penicillin and grown at 37 °C with 5% CO<sub>2</sub> (Thermo). MDA-MB-231 was cultured with L15 (Gibco,

(See figure on next page.)

**Fig. 5** SNHG1 acted as a ceRNA to enhance TERT expression by sponging miR-18b-5p. **a** Transfection efficacy of miR-18b-5p mimics in MDA-MB-468 and Hs578T cells. **b, c** Overexpression of miR-18b-5p downregulated TERT mRNA and protein expression. **d, e** miR-18b-5p inhibitor upregulated TERT mRNA and protein expression. **f, g** Overexpression of miR-18b-5p inhibited SNHG1 expression; however, downregulated miR-18b-5p promoted SNHG1 expression. **h** Silencing SNHG1 and inhibiting miR-18b-5p weakened the downregulation of TERT at the protein level in MDA-MB-468 and Hs578T cells. **i, j** A luciferase reporter assay was used to assess the interactions between miR-18b-5p and its binding sites or mutated binding sites in the 3' UTRs of TERT and SNHG1 in HEK293T cells. **k, l** siSNHG1-mediated restraint of cell proliferation and invasion abilities was partially rescued by co-transfection of miR-18b-5p inhibitor in Hs578T and MDA-MB-468 cells. **m** miR-18b-5p expression in Balb/C mice with snhg1 knockdown. Data are presented as the mean value from three independent experiments ± S.D. \**P* < 0.05; \*\**P* < 0.01; \*\*\**P* < 0.001; \*\*\*\**P* < 0.0001; NS no significance

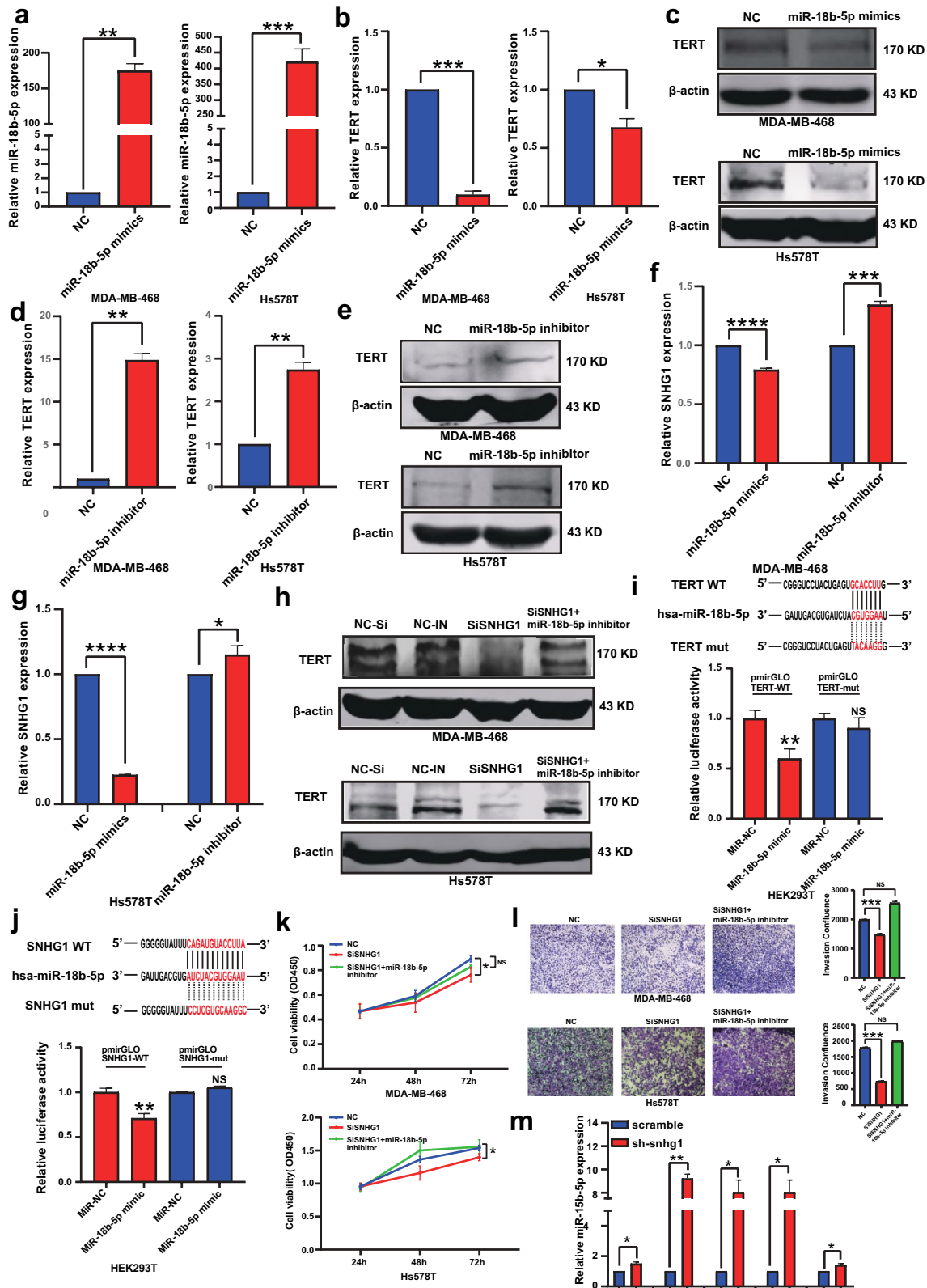


**Fig. 5** (See legend on previous page.)

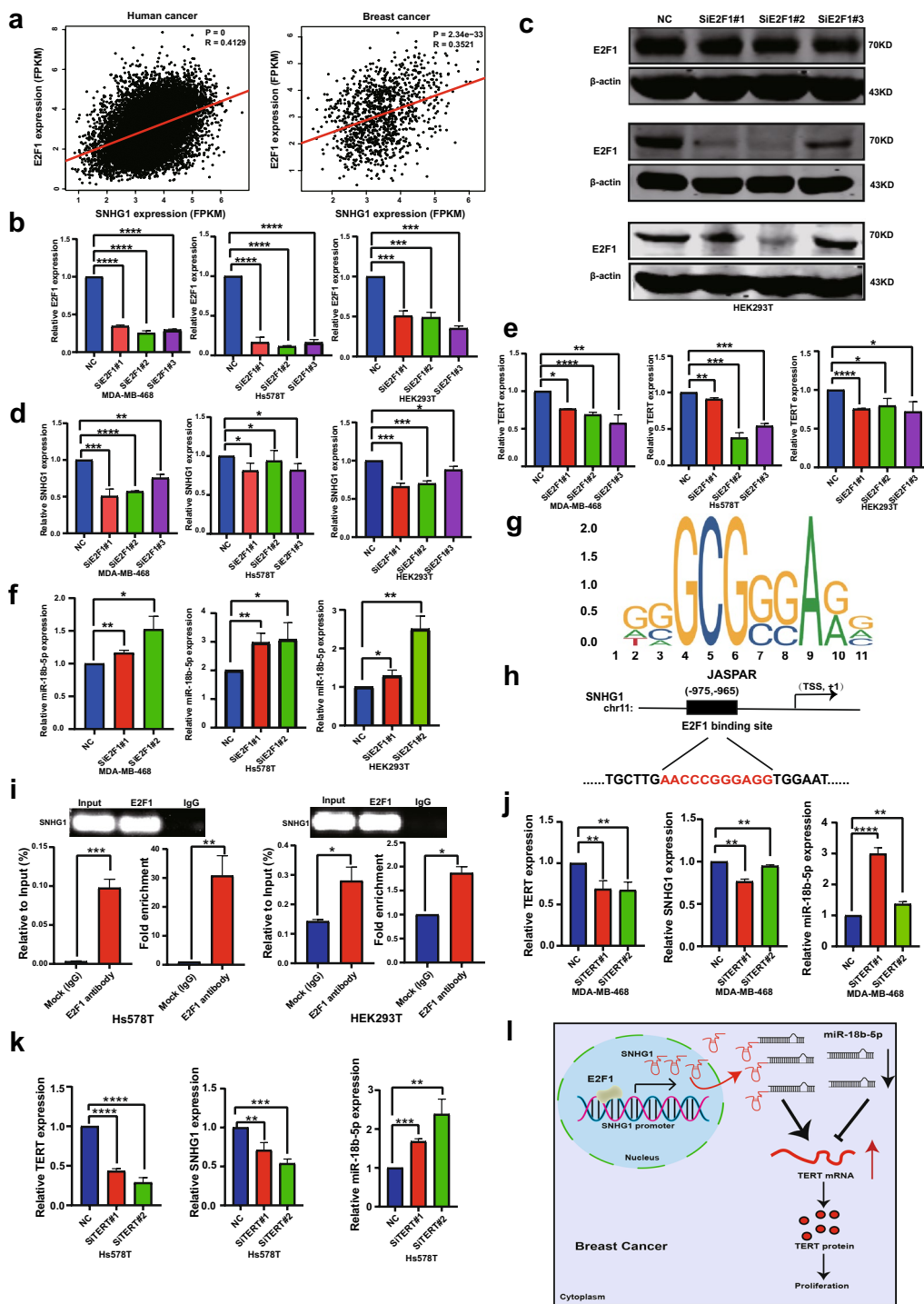


**Fig. 6** E2F1 promoted SNHG1 transcription. **a** TCGA data showed that E2F1 is positively correlated with SNHG1 in pan-cancer and in breast cancer. Knockdown efficacy of siE2F1 at mRNA (**b**) and protein (**c**) levels in MDA-MB-468, Hs578T, and HEK293T cells. **d** Knockdown of E2F1 downregulated SNHG1 expression. **e** Knockdown of E2F1 downregulated TERT mRNA expression. **f** Knockdown of E2F1 upregulated miR-18b-5p expression. **g** JASPAR predicted that E2F1 could bind with the promoter of SNHG1. **h** Schematic representation of the predicted E2F1 binding sites within the promoter of SNHG1. **i** Chromatin immunoprecipitation assay showed the binding of E2F1 and SNHG1 promoter region in Hs578T and HEK293T cells. **j, k** Silencing TERT could downregulate the expression of SNHG1 and upregulate the expression of miR-18b-5p. **l** Working model of the study. Data are presented as the mean value from three independent experiments  $\pm$  S.D. \* $P < 0.05$ ; \*\* $P < 0.01$ ; \*\*\* $P < 0.001$ ; \*\*\*\* $P < 0.0001$ ; NS no significance

Waltham, MA) medium and 10% FBS, 100  $\mu$ /mL penicillin and grown at 37 °C with air incubator (Thermo).

#### Patients and tissue specimens

Breast cancer tissues and paired normal tissues were obtained from Harbin Medical University Cancer Center (HMUCC). None of the patients received adjuvant chemotherapy, immunotherapy, or radiotherapy before surgery, and patients with recurrent tumors, metastatic disease, bilateral tumors, or other previous tumors were excluded. For RNA extraction, fresh tissue from individuals with breast cancer and normal controls was collected and stored at  $-80$  °C immediately resection. The expression level of SNHG1 and TERT were measured by RT-qPCR. This study was approved by the Ethics Committees of Harbin Medical University. Written informed consent was obtained from all subjects who participated in this study.

#### RNA extraction and RT-PCR

Total RNA samples from cells samples were isolated using Trizol reagent (Invitrogen, USA) according to manufacturer's protocols. Total RNA (0.5  $\mu$ g) was then reverse transcribed using Transcriptor First Strand cDNA Synthesis Kit (Roche, USA) to obtain cDNA. The SYBR Green PCR Master Mix Kit (Applied Biosystems, USA) was used to quantify the RNA levels using SYBR Green PCR Master Mix Kit, and the results were normalized against GAPDH and U6 expression levels using the  $2^{-\Delta\Delta CT}$  method. The RT-qPCR was performed on ABI StepOne Real-time PCR System (Applied Biosystems, USA). The primer sequences are as follows: SNHG1-F: 5'-AACTTCCCATAACTCCACTTC-3'; SNHG1-R: 5'-ACAACCAACACAGCAACAC-3'; TERT-F: 5'-CTGTACTTTGTCAAGGTGGATGTGA-3'; TERT-R: 5'-ACGTGTTCTGGGGTTTGATGATG-3'; Hsa-miR-18b-5p-F: 5'-CGGGCTAAGGTGCATCTAGTGC-3'; Hsa-miR-18b-5p-R: 5'-ATCCAGTGCAGGGTCCGAGG-3'; Hsa-miR-18b-5p-RT: 5'-GTCGTATCCAGTGCAGGGTCCGAGGTATTCGCACTGGATACGACCTAAC-3'; Hsa-U6-F: 5'-GCTTCGGCAGCATATACTAAAAT-3'; Hsa-U6-R: 5'-CGCTTCACGAATTTGCGTGTGCAT-3'; Hsa-U6-RT: 5'-CGCTTCACGAATTTGCGTGTGCAT-3';

Hsa-miR-18a-5p-F: 5'-GCGGGCTAAGGTGCATCTAGTGC-3'; Hsa-miR-18a-5p-R: 5'-ATCCAGTGCAGGTCCGAGG-3'; Hsa-miR-18a-5p-RT: 5'-GTCGTATCCAGTGCAGGGTCCGAGGTATTCGCACTGGATACGACCTATCT-3'; Hsa-miR-376a-3p-F: 5'-CGGGCCGATCATAGAGGAAAAT-3'; Hsa-miR-376a-3p-R: 5'-ATCAGTGCAGGGTCCGAGG-3'; Hsa-miR-376a-3p-RT: 5'-GTCGTATCCAGTGCAGGGTCCGAGGTATTCGCACTGGATACGACACGTGG-3'; Hsa-383-5p-F:

5'-GCGGGCAGATCAGAAGGTGATT-3'; Hsa-383-5p-R: 5'-ATCCAGTGCAGGGTCCGAGG-3'; Hsa-383-5p-RT: 5'-GTCGTATCCAGTGCAGGGTCCGAGGTATTCGCACTGGATACGACAGCCAC-3'; GAPDH-F: 5'-CATGTTTCGTATCCAGTGCAGGGTCCGAGGTATTCGCACTGGATACGACAGCCAC-3'; GAPDH-R: 5'-GGCATGGACTGTGGTTCATGAG-3'; E2F1-F: 5'-ACGTGACGTGTCAGGACCT-3'; E2F1-R: 5'-GATCGGGCCTTGTGCTCTT-3'; Mus-TERT-F: 5'-TCTACCGCACTTGGTTGCC-3'; Mus-TERT-R: 5'-CAGCACGTTTCTCTCGTTGC-3'.

#### Transfection of small interfering RNAs, miRNA mimics/inhibitors and plasmid

LncRNA SNHG1 short interfering RNA (siRNAs), Hsa-miR-18b-5p mimics and Hsa-miR-18b-5p inhibitor were synthesized by Ribo Co., Ltd. (Guangdong, China). SNHG1 plasmid (pcDNA3.1-SNHG1) was constructed by Shanghai GeneChem, Co. for SNHG1 overexpression. Cells were seeded in 6-well plate, when the cells grow 70–80% confluence for miRNA (100 nmol), siRNA (100 nmol), inhibitor (50 nmol) and SNHG1 overexpression plasmid (2000 ng) transfection. Cells were transfected using jetPRIME (Polyplus transfection). The sequences are as follows: si-control sense: UUCUCCGAACGUGUCACGUTT; si-SNHG1#1 sense: GGUUUGCUGUGUAUCACAUTT; si-SNHG1#2 sense: GACCUAGCUUGUUGCCAAUTT; si-E2F1#1 sense: GAGACCTCTTCGACTGTGA; si-E2F1#2 sense: CTATGAGACCTCACTGAAT; si-E2F1#3: GGGAGAAGTCACGCTATGA; si-TERT#1 sense: GAGCCAGTCTCACCTCAA; si-TERT#2 sense: GGAGCAAGTTGCAAA GCAT; si-TERT#3 sense: GAGTGACCGTGGTTTCTGT. Scrambled negative control mimics/inhibitor and microRNA (miR) 18b-5p-, miR-383-5p were purchased from Invitrogen (Invitrogen, CA, USA) and had the following sequences: Hsa-miR-18b-5p mimics sense: UAA GGUGCAUCUAGUGCAGUUAG antisense: AACUGCACUAGAUGCACCUUAAU; Hsa-miR-18b-5p inhibitor sense: CUAACUGCACUAGAUGCACCUUA; Hsa-miR-383-5p mimics sense: AGAUCAGAAGGUGAUUGU GGCU antisense: CCACAAUCACCUUCUGAUCUUU; has-18b-5p inhibitor sense: CUAACUGCACUAGAU GCACCUUA.

#### Lentiviral transfection

The full-length RNAi sequences and antisense were amplified by PCR and cloned into Lentiviral particles had puromycin selection and were constructed and packaged by Shanghai GeneChem, Co., Ltd. For lentiviral transfection, moderate lentiviruses were used to infect 4T1 cells in a 6-well plate with 4–6  $\mu$ g/mL polybrene (#107689, Sigma). The infected cells were then subjected to selection with 1  $\mu$ g/mL puromycin (#540411, Calbiochem,

USA) cultured for several days. The stable knockdown of *snhg1* was examined by RT-PCR. The sequence of lenti-virus as follows: sh-*snhg1*#1: CTGGTGACAAATCTCAGGCAT; sh-*snhg1*#2: GTGGTTCATCTCAAAGCCCTT; sh-*snhg1*#3: AAGGATAGGAACAGAAATCAT.

#### Cell viability assay

The viability of treated cells was estimated by a Cell Counting Kit-8 (CCK-8; Dojindo Laboratories, Kumamoto, Japan) assay according to the manufacturer's instructions and as previously described [47]. Briefly, cells were plated at a density of  $5 \times 10^3$  cells/well with 100  $\mu$ L of DMEM + 10% FBS in 96-well microtiter plates. 10  $\mu$ L CCK-8 solution was added to each well which including 100  $\mu$ L DMEM medium, and then the plate was incubated at 37 °C for 60 min. Next, the absorbance of each well was measured by a microplate reader at a wavelength of 450 nm. Medium containing 10% CCK-8 served as a control.

#### Colony formation assay

$1 \times 10^3$  cells were seeded in 6-well plate and cultured in medium containing 10% FBS for 14 days.

Discard the culture medium, PBS wash the 6-well plate three times. Colonies were fixed with methanol for 40 min, then 500  $\mu$ L of 5% crystal violet (Sigma-Aldrich, St. Louis, MO, USA) were added to each well for 30 min. After staining, colonies were gently washed and counted.

#### Wound healing assay

Cells were seeded in 6-well plate, transfected with siRNAs or miRNA mimics according to previous method. When cell confluence reached 100%, 10  $\mu$ L pipette was used to scratch on the bottom of the 6-well plate. The scratched cells were washed away. Then taking photos in 0 h, 24 h, 48 h.

#### Transwell invasion assay

Transwell invasion assay was performed using a Transwell plate (Corning, New York, USA) was coated with Matrigel (Sigma-Aldrich, USA).  $5 \times 10^4$  cells in serum-free medium were suspended in upper chamber with Matrigel. Medium containing 20% FBS (Seratech, PAN) was added to the bottom chamber. After incubating at 37 °C for 48 h. Then discard the culture medium, cells that invaded to the lower side of the Transwell were fixed with methanol, stained with 0.5% crystal violet and imaged under a microscope. Image J was used to count the number of cells.

#### Animal experiment

Animal experiments were approved by the Medical Experimental Animal Care Commission of Harbin

Medical University. 4–5 weeks old female Balb/C mice were purchased from Animal Center of the Second Affiliated Harbin Medical University. 4T1 cells stably expressing sh-scramble and sh-*snhg1*#3 were resuspended with DMEM medium. Then 100  $\mu$ L of serum-free medium containing  $5 \times 10^4$  cells were injected into the right mammary fat pad. The tumor volume was measured with a caliper every 2 days beginning on day 6 days after cell implantation. BIBR1532 was administrated intraperitoneally (i.p.) at a dose of 1.5 mg/kg for 2 weeks. The tumor volume was calculated using the formula tumor volume =  $1/2$  (length  $\times$  width<sup>2</sup>). Then the mice were euthanized, the weight of tumors in mouse were measured. Then, half of the tumors was extracted protein and the other half was extracted RNA.

#### Western blot assay

Cells were lysed with lysis buffer which containing 150 mmol/L NaCl, 1% Triton X-100, 5 mmol/L EDTA, 5000 U/mL aprotinin, 20 mg/mL leupeptin, 1 mmol/L phenyl-methylsulfonyl fluoride, 2 mmol/L sodium orthovanadate, 50 mmol/L NaF, 5% glycerol, 10 mmol/L Tris-HCl (pH 7.4), and 2% SDS. Then ultrasonic crusher was used to broken cell nucleus. After centrifugation at  $13,500 \times g$  for 30 min, supernatant was collected. Next, protein concentrations were tested by BCA protein assay kit (#p0010; Beyotime, Shanghai, China). Then these proteins were separated by SDS-PAGE, followed by electroblotting onto a nitrocellulose membrane, which was blocked with 5% nonfat milk in 0.1% Tween 20-TBS overnight at 4 °C. The membrane was incubated with primary antibody against TERT (#sc-377511; Santa cruz biotechnology), E2F1 antibody (#3742; Cell Signaling Technology) and  $\beta$ -actin (#sc-377511; Santa cruz biotechnology). After washing with Tween 20/TBS (TBST), the membrane was incubated with horseradish peroxidase-conjugated secondary antibodies for 1 h in room temperature. After washing with Tween 20/PBS (PBST), protein bands on the membrane were visualized by an enhanced chemiluminescence Western blotting detection system (Western Lightning; Perkin-Elmer, Norwalk, CT).

#### Dual-luciferase reporter gene assay

We cloned the full length of the 3' untranslated regions (UTRs) of human SNHG1 and TERT to generate reporter vectors with miRNA binding sites. The full length of 3' UTRs of human SNHG1 and TERT were amplified by PCR and cloned into psi-CHECK-2 luciferase expression vector that contained Not1-XhoI sites. HEK293T cells were chosen to perform this assay. When 293 T reached 40–50% confluence, JetPRIME was used to transfect HEK293T with 20  $\mu$ mol/L Hsa-miR-18b-5p mimics or negative control mimics and 0.5 mg of plasmid. The

luciferase activities were measured 48 h after transfection using a dual-luciferase reporter assay kit (#E1910, Promega, USA) and a luminometer (GloMax 20/20, Promega, USA).

#### Cytoplasmic-nuclear RNA fractionation

Cytoplasmic and nuclear RNA extraction were separated using the cytoplasmic and nuclear RNA purification kit (#21000, NORGEN) as directed by the manufacturer. We harvested  $3 \times 10^6$  cells (HEK293T, MDA-MB-468, and Hs578T), washed them with ice-cold PBS, and then resuspended these cells in the ice-cold cytoplasmic Lysis Buffer J for 5 min on ice. Then lysates were centrifuged at  $13,500 \times g$  for 10 min at 4 °C. The supernatant was collected as the cytoplasmic fraction, the remaining lysates was collected as the nuclear fraction. Finally, cytoplasm RNA and nucleus RNA were successfully separated. Then, the expression levels of GAPDH, U1 and SNHG1 in cytoplasm or nucleus were detected by RT-PCR.

#### Chromatin immunoprecipitation (ChIP)

Chromatin immunoprecipitation (ChIP) assays were performed using the ChIP Assay Kit (#p2078; Beyotime, Shanghai, China) according to the manufacturer's protocol.  $2 \times 10^7$  cells were crosslinked with 1% formaldehyde, and this reaction was terminated after 20 min by the addition of glycine at a final concentration of 0.125 M. DNA was immunoprecipitated from sonicated cell lysates using an E2F1 antibody; IgG (BD Biosciences, San Diego, CA, USA) served as the negative control. Protein A/G Plus-agarose was purchased from Santa Cruz Biotechnology (#sc-2003). RNase A as Proteinase K treatment, immunoprecipitated DNA was extracted by DNA purification kit (Beyotime, Shanghai, China). The immunoprecipitated DNA was subjected to PCR to amplify the E2F1 promoter binding sites. The amplified fragments were then analyzed on an agarose gel. Chromatin (1%) prior to immunoprecipitation was used as the input control. The primer sequences of binding site between E2F1 and SNHG1 were as follows: SNHG1-F: 5'-CAGGAGAAT TGCTTGAACCCG-3'; SNHG1-R: 5'-TGGCCCGAT CTCAGCTCACT-3'.

#### Nucleic acid electrophoresis

The DNA PCR products were investigated using 1% agarose gel electrophoresis with TAE running buffer. DNA was separated by electrophoresis at 100 V for 30 min. The DNA marker was Marker L (50–500 bp) (Sango Biotech, China). The bands were examined by UV irradiation (Biorad).

#### Statistical analyses

The expression of SNHG1 in cancer tissues compared with normal tissues were tested by a paired t-test. Kaplan–Meier method and log-rank test were used to evaluate the survival difference between patients with high SNHG1 expression and low SNHG1 expression. The differences in the results of the in vitro and in vivo experiments between groups were analyzed using Student's t-test. All the experiments were performed independently in triplicate. All statistical tests were two-sided, and  $P < 0.05$  indicated statistical significance. Statistical analysis was performed using 332R.3.4 graphics software and GraphPad Prism software (GraphPad Software, USA).

#### Abbreviations

ACC: Adrenocortical carcinoma; BLCA: Bladder urothelial carcinoma; BRCA: Breast carcinoma; CCK-8: Cell counting Kit-8; ceRNA: Competing endogenous RNA; CESC: Cervical and endocervical cancers; ChIP: Chromatin immunoprecipitation; CHOL: Cholangiocarcinoma; COAD: Colon adenocarcinoma; DEG: Differentially expressed gene; DSS: Disease specific survival; EMT: Epithelial mesenchymal transformation; ESCA: Esophageal carcinoma; HNSC: Head and neck squamous cell carcinoma; GEPIA: Gene Expression Profiling Interactive Analysis; KICH: Kidney chromophobe; KIRC: Kidney renal clear cell carcinoma; KIRP: Kidney renal papillary cell carcinoma; LIHC: Liver hepatocellular carcinoma; LncRNA: Long noncoding RNAs; LUAD: Lung adenocarcinoma; LUSC: Lung squamous cell carcinoma; miRNA: MicroRNA; ORF: Open reading frame; OS: Overall survival; PCPG: Pheochromocytoma and paraganglioma; PRAD: Prostate adenocarcinoma; READ: Rectum adenocarcinoma; RFS: Relapse free survival; SARC: Sarcoma; siRNA: Short interfering RNA; SNHG1: Small nucleolar RNA host gene1; STAD: Stomach adenocarcinoma; TCGA: The Cancer Genome Atlas; TERC: Telomerase RNA component; TERT: Telomerase reverse transcriptase; TF: Transcription factor; THCA: Thyroid carcinoma; TNBC: Triple negative breast cancer; UCEC: Uterine corpus endometrial carcinoma; UTRS: Untranslated regions.

#### Supplementary Information

The online version contains supplementary material available at <https://doi.org/10.1186/s13578-021-00675-5>.

**Additional file 1: Figure S1. a–c** Higher expression level of SNHG1 was associated with poor overall survival, disease specific survival and progression free interval in UCEC. **d–f** Higher expression level of SNHG1 was associated with poor disease specific survival, progression free interval and disease-free interval in LIHC. **g–i** Higher expression level of SNHG1 was associated with poor overall survival, disease free interval and progression free interval in PRAD. **j–k** Higher expression level of SNHG1 was associated with poor overall survival and progression free interval in ACC. **l–o** Higher expression of SNHG1 was correlated with poor OS in LIHC, KIRC, SARC and UCEC.

**Additional file 2: Figure S2.** CCK-8 (**a**), wound healing (**b**) and colony formation assays (**c**) were performed to identify that silencing of TERT inhibited tumor cell proliferation and colony formation and suppressed tumor cell migration and invasion in MDA-MB-468 and Hs578T.

**Additional file 3: Table S1.** The clinical pathology information of the breast cancer tissues in the TCGA analysis for SNHG1 expression level.

**Additional file 4: Table S2.** SNHG1 expression and prognosis of human pan-cancer in TCGA database.

**Additional file 5: Table S3.** Regarding the primary samples ( $n = 5$ ) validating the SNHG1 and TERT expression, patient demographic data were provided.

**Additional file 6: Table S4.** The relationship between expression of SNHG1 and TERT of human pan-cancer in TCGA database.

**Additional file 7: Table S5.** The expression profile of coding gene in breast cancer was extracted from TCGA BRCA expression profile.

**Additional file 8: Table S6.** TargetScan, and starBase databases to predict the possible miRNAs that could interact with both SNHG1 and TERT, simultaneously.

**Additional file 9: Table S7.** PROMO database was used to predict potential transcription factors (TFs) that could bind to the SNHG1 promoter.

**Additional file 10: Table S8.** The relationship between expression of E2F1 and SNHG1 of human pan-cancer in TCGA database.

**Additional file 11: Table S9.** JASPAR database was used to predict the potential binding site between E2F1 and SNHG1 promoter.

### Acknowledgements

None.

### Authors' contributions

Conceptualization, XSP and KYJ; data curation, KYJ, LL, LJN, YYL, ZL and ZX; data analysis, WL, YYL; writing-original draft preparation, KYJ; writing-review and editing, PD, XSP, WQ; funding acquisition, PD, XSP and WQ. All authors read and approved the final manuscript.

### Funding

This work was supported by funding from the Project Nn10 of Harbin Medical University Cancer Hospital (Grant Number Nn102017-02), the National Natural Science Foundation of China (Grant Numbers 82072904, 81872149, 81972706, 82103325), Outstanding Youth Project of Heilongjiang Provincial Natural Science Foundation (Grant Number YQ2019H027), Distinguished Young Scholars of Harbin Medical University Cancer Hospital (Grant Number JCQN2018-03), Yong Elite Training Foundation Grant of Harbin Medical University Cancer Hospital (Grant Number JY2016-02) and Haiyan Fund Project of Harbin Medical University Cancer Hospital (Grant number JJQN 2018-10).

### Availability of data and materials

All remaining data are availability within the article and Additional files, or available from the authors upon request.

### Declarations

#### Ethics approval and consent to participate

All animal experiments were performed in accordance with the National Institutes of Health guide for the care and use of Laboratory animals and protocols approved by the Animal Ethics Committee of Harbin Medical University of Medicine and Health Sciences. The use of breast cancer tissue samples was approved and authorized by the Ethics Committee of Harbin Medical University of Medicine and Health Sciences. Both the patient and his family members have signed the informed notice and informed consent of tissue use. All behaviors conform to laws, regulations and rules.

#### Consent for publication

All author shave agreed to publish this manuscript.

#### Competing interests

The authors declare no conflict of interest.

#### Author details

<sup>1</sup>Department of Breast Surgery, Harbin Medical University Cancer Hospital, Harbin 150040, China. <sup>2</sup>Heilongjiang Academy of Medical Sciences, Harbin, China.

Received: 27 February 2021 Accepted: 3 August 2021

Published online: 31 August 2021

### References

- Lee S, Kopp F, Chang TC, Sataluri A, Chen B, Sivakumar S, et al. Noncoding RNA NORAD regulates genomic stability by sequestering PUMILIO proteins. *Cell*. 2016;164(1–2):69–80.
- Niazi F, Valadkhan S. Computational analysis of functional long noncoding RNAs reveals lack of peptide-coding capacity and parallels with 3' UTRs. *RNA*. 2012;18(4):825–43.
- Zhao J, Song X, Wang K. IncScore: alignment-free identification of long noncoding RNA from assembled novel transcripts. *Sci Rep*. 2016;6(1):1–12.
- Jia H, Osak M, Bogu GK, Stanton LW, Johnson R, Lipovich L. Genome-wide computational identification and manual annotation of human long noncoding RNA genes. *RNA*. 2010;16(8):1478–87.
- Saha A, Bhattacharya S, Bhattacharya A. Serum stress responsive gene EhsIncRNA of *Entamoeba histolytica* is a novel long noncoding RNA. *Sci Rep*. 2016;6(1):1–9.
- Gibb EA, Brown CJ, Lam WL. The functional role of long non-coding RNA in human carcinomas. *Mol Cancer*. 2011;10(1):1–17.
- Spizzo R, Almeida MI, Colombatti A, Calin GA. Long non-coding RNAs and cancer: a new frontier of translational research? *Oncogene*. 2012;31(43):4577–87.
- Bhan A, Soleimani M, Mandal SS. Long noncoding RNA and cancer: a new paradigm. *Cancer Res*. 2017;77(15):3965–81.
- Verhoeven RJA, Tong S, Mok BW, Liu J, He S, Zong J, et al. Epstein-Barr virus BART long non-coding RNAs function as epigenetic modulators in nasopharyngeal carcinoma. *Front Oncol*. 2019;9:1120.
- Zhang J, Sui S, Wu H, Zhang J, Zhang X, Xu S, et al. The transcriptional landscape of lncRNAs reveals the oncogenic function of LINC00511 in ER-negative breast cancer. *Cell Death Dis*. 2019;10(8):599.
- Salmena L, Poliseno L, Tay Y, Kats L, Pandolfi PP. A ceRNA hypothesis: the Rosetta Stone of a hidden RNA language? *Cell*. 2011;146(3):353–8.
- Achkar NP, Cambiagno DA, Manavella PA. miRNA biogenesis: a dynamic pathway. *Trends Plant Sci*. 2016;21(12):1034–44.
- Karreth FA, Tay Y, Perna D, Ala U, Tan SM, Rust AG, et al. In vivo identification of tumor-suppressive PTEN ceRNAs in an oncogenic BRAF-induced mouse model of melanoma. *Cell*. 2011;147(2):382–95.
- Tay Y, Kats L, Salmena L, Weiss D, Tan SM, Ala U, et al. Coding-independent regulation of the tumor suppressor PTEN by competing endogenous mRNAs. *Cell*. 2011;147(2):344–57.
- Yan Y, Fan Q, Wang L, Zhou Y, Li J, Zhou K. LncRNA Snhg1, a non-degradable sponge for miR-338, promotes expression of proto-oncogene CST3 in primary esophageal cancer cells. *Oncotarget*. 2017;8(22):35750–60.
- Li J, Zhang Z, Xiong L, Guo C, Jiang T, Zeng L, et al. SNHG1 lncRNA negatively regulates miR-199a-3p to enhance CDK7 expression and promote cell proliferation in prostate cancer. *Biochem Biophys Res Commun*. 2017;487(1):146–52.
- Wang Q, Li Q, Zhou P, Deng D, Xue L, Shao N, et al. Upregulation of the long non-coding RNA SNHG1 predicts poor prognosis, promotes cell proliferation and invasion, and reduces apoptosis in glioma. *Biomed Pharmacother*. 2017;91:906–11.
- Liu L, Shi Y, Shi J, Wang H, Sheng Y, Jiang Q, et al. The long non-coding RNA SNHG1 promotes glioma progression by competitively binding to miR-194 to regulate PHLDA1 expression. *Cell Death Dis*. 2019;10(6):463.
- Cui L, Dong Y, Wang X, Zhao X, Kong C, Liu Y, et al. Downregulation of long noncoding RNA SNHG1 inhibits cell proliferation, metastasis, and invasion by suppressing the Notch-1 signaling pathway in pancreatic cancer. *J Cell Biochem*. 2019;120(4):6106–12.
- Pei X, Wang X, Li H. LncRNA SNHG1 regulates the differentiation of Treg cells and affects the immune escape of breast cancer via regulating miR-448/IDO. *Int J Biol Macromol*. 2018;118(Pt A):24–30.
- Xiong X, Feng Y, Li L, Yao J, Zhou M, Zhao P, et al. Long noncoding RNA SNHG1 promotes breast cancer progression by regulation of LMO4. *Oncol Rep*. 2020;43(5):1503–15.
- Li J, Zeng T, Li W, Wu H, Sun C, Yang F, et al. Long non-coding RNA SNHG1 activates HOXA1 expression via sponging miR-193a-5p in breast cancer progression. *Aging*. 2020;12(11):10223–34.
- Zheng S, Li M, Miao K, Xu H. SNHG1 contributes to proliferation and invasion by regulating miR-382 in breast cancer. *Cancer Manag Res*. 2019;11:5589–98.

24. Blackburn EH. Switching and signaling at the telomere. *Cell*. 2001;106(6):661–73.
25. Moyzis RK, Buckingham JM, Cram LS, Dani M, Deaven LL, Jones MD, et al. A highly conserved repetitive DNA sequence, (TTAGGG)<sub>n</sub>, present at the telomeres of human chromosomes. *Proc Natl Acad Sci USA*. 1988;85(18):6622–6.
26. Makarov VL, Hirose Y, Langmore JP. Long G tails at both ends of human chromosomes suggest a C strand degradation mechanism for telomere shortening. *Cell*. 1997;88(5):657–66.
27. Greider CW, Blackburn EH. A telomeric sequence in the RNA of tetrahymena telomerase required for telomere repeat synthesis. *Nature*. 1989;337(6205):331–7.
28. Lendvay TS, Morris DK, Sah J, Balasubramanian B, Lundblad V. Senescence mutants of *Saccharomyces cerevisiae* with a defect in telomere replication identify three additional EST genes. *Genetics*. 1996;144(4):1399–412.
29. Lingner J, Cech TR. Purification of telomerase from *Euplotes aediculatus*: requirement of a primer 3' overhang. *Proc Natl Acad Sci USA*. 1996;93(20):10712–7.
30. Cong YS, Wright WE, Shay JW. Human telomerase and its regulation. *Microbiol Mol Biol Rev*. 2002;66(3):407–25 (**table of contents**).
31. Li C, Wu MY, Liang YR, Wu XY. Correlation between expression of human telomerase subunits and telomerase activity in esophageal squamous cell carcinoma. *World J Gastroenterol*. 2003;9(11):2395–9.
32. Yi X, Tesmer VM, Savre-Train I, Shay JW, Wright WE. Both transcriptional and posttranscriptional mechanisms regulate human telomerase template RNA levels. *Mol Cell Biol*. 1999;19(6):3989–97.
33. Kim NW, Piatyszek MA, Prowse KR, Harley CB, West MD, Ho PL, et al. Specific association of human telomerase activity with immortal cells and cancer. *Science*. 1994;266(5193):2011–5.
34. Cukusic A, Vidacek NS, Sopta M, Rubelj I. Telomerase regulation at the crossroads of cell fate. *Cytogenet Genome Res*. 2008;122(3–4):263–72.
35. Siegel RL, Miller KD, Jemal A. Cancer statistics, 2016. *CA Cancer J Clin*. 2016;66(1):7–30.
36. Chen W. Cancer statistics: updated cancer burden in China. *Chin J Cancer Res*. 2015;27(1):1.
37. Breast Cancer Treatment (Adult) (PDQ(R)): Patient Version, in PDQ Cancer Information Summaries. 2002: Bethesda (MD).
38. Elkak A, Mokbel R, Wilson C, Jiang WG, Newbold RF, Mokbel K. hTERT mRNA expression is associated with a poor clinical outcome in human breast cancer. *Anticancer Res*. 2006;266C:4901–4.
39. Nagy A, Lanczky A, Menyhart O, Györfy B. Validation of miRNA prognostic power in hepatocellular carcinoma using expression data of independent datasets. *Sci Rep*. 2018;8(1):9227.
40. Pascolo E, Wenz C, Lingner J, Haeufel N, Pripke H, Kauffmann I, et al. Mechanism of human telomerase inhibition by BIBR1532, a synthetic, non-nucleosidic drug candidate. *J Biol Chem*. 2002;277(18):15566–72.
41. Adams BD, Parsons C, Walker L, Zhang WC, Slack FJ. Targeting noncoding RNAs in disease. *J Clin Invest*. 2017;127(3):761–71.
42. Hua K, Deng X, Hu J, Ji C, Yu Y, Li J, et al. Long noncoding RNA HOST2, working as a competitive endogenous RNA, promotes STAT3-mediated cell proliferation and migration via decoying of let-7b in triple-negative breast cancer. *J Exp Clin Cancer Res*. 2020;39(1):58.
43. Sun Y, Wei G, Luo H, Wu W, Skogerbo G, Luo J, et al. The long noncoding RNA SNHG1 promotes tumor growth through regulating transcription of both local and distal genes. *Oncogene*. 2017;36(49):6774–83.
44. Yuan X, Larsson C, Xu D. Mechanisms underlying the activation of TERT transcription and telomerase activity in human cancer: old actors and new players. *Oncogene*. 2019;38(34):6172–83.
45. Rashid F, Shah A, Shan G. Long non-coding RNAs in the cytoplasm. *Genom Proteom Bioinform*. 2016;14(2):73–80.
46. Mizuno H, Kitada K, Nakai K, Sarai A. PrognoScan: a new database for meta-analysis of the prognostic value of genes. *BMC Med Genom*. 2009;2(1):1–11.
47. Kholodenko BN, Demin OV, Moehren G, Hoek JB. Quantification of short term signaling by the epidermal growth factor receptor. *J Biol Chem*. 1999;274(42):30169–81.

## Publisher's Note

Springer Nature remains neutral with regard to jurisdictional claims in published maps and institutional affiliations.

Ready to submit your research? Choose BMC and benefit from:

- fast, convenient online submission
- thorough peer review by experienced researchers in your field
- rapid publication on acceptance
- support for research data, including large and complex data types
- gold Open Access which fosters wider collaboration and increased citations
- maximum visibility for your research: over 100M website views per year

At BMC, research is always in progress.

Learn more [biomedcentral.com/submissions](https://biomedcentral.com/submissions)

